Indicator Supraparticles for Smart Gasochromic Sensor Surfaces Reacting Ultrafast and Highly Sensitive

Susanne Wintzheimer, Maximilian Oppmann, Martin Dold, Carolin Pannek, Marie-Luise Bauersfeld, Michael Henfling, Sabine Trupp, Benedikt Schug, and Karl Mandel*

The detection of toxic gases, such as NH₃ and CO, in the environment is of high interest in chemical, electronic, and automotive industry as even small amounts can display a health risk for workers. Sensors for the real-time monitoring of these gases should be simple, robust, reversible, highly sensitive, inexpensive and show a fast response. The indicator supraparticles presented herein can fulfill all of these requirements. They consist of silica nanoparticles, which are assembled to supraparticles upon spray-drying. Sensing molecules such as Reichardt's dye and a binuclear rhodium complex are loaded onto the microparticles to target NH₃ and CO detection, respectively. The spray-drying technique affords high flexibility in primary nanoparticle size selection and thus, easy adjustment of the porosity and specific surface area of the obtained micrometer-sized supraparticles. This ultimately enables the fine-tuning of the sensor sensitivity and response. For the application of the indicator supraparticles in a gas detection device, they can be immobilized on a coating. Due to their microscale size, they are large enough to poke out of thin coating layers, thus guaranteeing their gas accessibility, while being small enough to be applicable to flexible substrates.

1. Introduction

The monitoring of gases in the environment is of high interest in chemical, electronic, and automotive industry.[1] The detection

of both, NH₃ and CO, is compulsory for these industrial fields, as already small amounts of these gases can display a health risk for their workers.[2–6] The detection of ammonia vapors is also required to guarantee a high product quality in semiconductor manufacturing[7,8] or to control the spoiling of food.[2,9] Carbon monoxide, which is produced by incomplete burning of natural gas or carbon-based fuels, is additionally of utmost importance in the field of fire detection.[1,5,6]

Sensors for the real-time monitoring of NH₃ and CO gases should be simple, robust, reversible, highly sensitive, and inexpensive and show a fast response.[2,7,10] Electrochemical sensors have commonly been employed for this purpose.[2,6,11] However, this technology usually comes with disadvantages such as the need for a reference electrode, sensor irreversibility or susceptibility to temperature and pressure.[2,6,7] One strategy to avoid these downsides is to use optical sensors based on chemical sensing molecules, which are carried by a support material.

Potential optical sensing molecules are functional dyes, displaying a change in absorbance or fluorescence at a certain wavelength, when they come into contact with a specific gas.[12] For the detection of gaseous ammonia or amine vapors, the solvatochromic Reichardt's betaine dye 2,6-diphenyl-4-(2,4,6-triphenyl-*N*-pyridinio)-phenolate has already been extensively studied.[13–17] The Reichardt's dye turns pink/violet when it dehydrates due to contact with ammonia vapors. However, in presence of air (i.e., atmospheric water), the color readily fades away. This reversible color change is not affected by other polar or nonpolar substances.[14] For the use as CO sensing molecules, binuclear rhodium complexes have been recently proposed.[5,6,18,19] These compounds show a reversible, fast, and selective reaction toward carbon monoxide.[19]

A wise selection of the support material for optical sensing molecules in solid state is crucial for the later sensor performance. Sensor parameters, such as response time and water cross-sensitivity, can be manipulated by the support.[17] The support material should further provide transparency in the UV–vis range, mechanical and chemical stability, as well as a high surface area, high pore volume, and adjustable pore

Dr. S. Wintzheimer, Dr. K. Mandel
Chair of Chemical Technology of Materials Synthesis
Julius-Maximilians-University Würzburg
Röntgenring 11, 97070 Würzburg, Germany
E-mail: karl-sebastian.mandel@isc.fraunhofer.de
M. Oppmann, B. Schug, Dr. K. Mandel
Fraunhofer Institute for Silicate Research ISC
Neunerplatz 2, 97082 Würzburg, Germany
Dr. M. Dold, Dr. C. Pannek, Dr. M.-L. Bauersfeld
Fraunhofer Institute for Physical Measurement Techniques IPM
Heidenhofstrasse 8, 79110 Freiburg, Germany
M. Henfling, Dr. S. Trupp
Fraunhofer Institute for Microsystems and Solid State Technologies EMFT
Hansastrasse 27 d, 80686 München, Germany

ADVANCED
SCIENCE NEWS
www.advancedsciencenews.com

Particle
& Particle Systems Characterization
www.particle-journal.com

sizes.[7,13–15,20] Mesoporous silica materials are candidates to address these requirements and have therefore been extensively studied as supports for gas phase chemical sensors.[2,7,13–15,20]

Supraparticles[21] consisting of individual silica nanoparticles present a novel mesoporous sensor support. These micrometer sized hierarchical particles, which are assembled upon spray-drying, have a raspberry-like appearance.[21–23] The spray-drying technique affords high flexibility in terms of building block selection (comparable to a toolbox), i.e., it is possible to readily select the primary particle size or to combine various sizes within one supraparticle. By choosing differently sized silica nanoparticle building blocks, the pore and void structure of the supraparticle can be controlled and the specific surface area adjusted.[23] Furthermore, it has been shown that the entire surface of the nanoparticles within the microparticle is nearly fully accessible by small gas molecules[23] resulting in very high specific surface areas, which is highly convenient for the use as sensor support. The raspberry-like supraparticles can be integrated into coatings yielding mole-hill structures as the micrometer-sized particles display the ideal size to poke out of a thinner coating layer.[24] This enables direct contact of these sensor support particles to the measured gas independent of the matrix (e.g., coating) material. At the same time, this setup renders the coating of flexible objects such as foils with a mesoporous sensor support possible.

The herein described sensors consist of raspberry-like silica supraparticles as support matrix for either Reichardt's dye or binuclear rhodium complexes for the detection of NH_3 or CO gas, respectively. These novel supraparticle sensors can meet all of the before mentioned criteria of an ideal sensor. Their setup is simple, their production is inexpensive and upscalable, and they can be incorporated in surface coatings, which have been shown as proof of principle. Their sensitivity can be readily adjusted and their colorimetric changes can be observed by the "naked eye," even at low analyte concentrations.

2. Results and Discussion

2.1. Composition of Supraparticles as Support Matrix

Herein, four different sizes of primary silica nanoparticle building blocks were assembled to supraparticles upon spray-drying. **Figure 1** depicts the microparticles in form of principal sketches of the particle structures either composed of a single type of primary silica nanoparticles sized 7, 10, 35, and 95 nm, as well as mixtures of 10 nm with 95 nm particles (with weight ratios of 1:9, 5:5, and 9:1) along with their nomenclature. The measured specific surface area, average pore diameter, and total pore volume determined by gas adsorption and calculated based on the Brunauer, Emmett, and Teller (BET) model, the Barret–Joyner–Halenda (BJH) analysis, and the Gurvich rule, respectively, are shown. Scanning electron microscopy (SEM) images display the microparticle shape as well as their surface structures.

It can be seen that by changing the primary silica nanoparticle size, the specific surface area of the particles can be varied from about 46 to about 166 $m^2 g^{-1}$, while the average pore diameter ranges from 37 to 160 Å and the total pore volume from 0.125 to 0.185 $cm^3 g^{-1}$. These three values are modified

by the assembly structure, as well as the packing density of one or two nanoparticle types in the microparticle. This is why the smallest size in primary nanoparticles does not automatically lead to the highest specific surface area of Particle A, which would be expected for nonassembled nanoparticles. The higher surface area and smaller pore diameter of Particle G compared to Particle B can also be only explained by the assembly structure of Particle G and not by the primary nanoparticle sizes.

2.2. CO Sensing by Indicator Supraparticles

For CO gas detection, the silica supraparticles as support matrix were loaded with a binuclear rhodium complex (further information in the Experimental Section). This complex was presented in more details in refs. [18] and [19]. Integrated into the silica-based supraparticles, the rhodium complex will show a color change from violet to yellow in presence of CO (**Figure 2**a), which is caused by a reversible two-step ligand exchange of the acetic acid by CO.[18,19] Reflectance spectra are measured using a Harrick Praying Mantis[25] diffuse reflectance accessory seated inside the sample compartment of a Perkin Elmer Lambda 900 UV–vis spectrometer (simplified in Figure 2b).

As soon as the CO target gas is released, the relative change in reflection intensity due to a color shift can be determined. Figure 2c depicts the relative change in reflection intensity at 470 nm of binary rhodium complex containing Particles A to D during 100 ppm CO gas exposure over 15 min, while Figure 2d displays the sensor response at 470 nm within the first 60 s of CO exposure. The reversibility of the sensor's color change is shown in Figure S1 in the Supporting Information.

For the evaluation of the gas detection measurements, one has to keep in mind that all particles (A to G) contain the same amount of binuclear rhodium complex, as for the loading procedure the sensor molecule concentration was set well below the adsorption saturation limit of the supraparticles. This is why the gas detection by the indicator supraparticles, i.e., the relative change in reflection, is only influenced by the intraparticle structure of the microparticles. Thus, this supraparticle structure has a direct effect on the gas penetration into the particle, adsorption of gas within the particle structure, and the interaction with the indicator molecule. It was expected that a large pore diameter and a high pore volume may be favorable for gas penetration and therefore, for the gas sensing properties. Comparing the specific surface area, the average pore diameter and the total pore volume with the relative changes in reflection caused by CO exposure for 15 min (Figure 2c) reveals that it is apparently the pore diameter, which mainly influences the sensing properties. Thus, the sensitivity of Particles C and D is superior compared to Particles A and B. However, the reason that Particle B reacts more sensitive than Particle A must be the higher specific surface area. As the reflection measurement is a surface sensitive technique, only the upper nanoparticle layers within a microparticle most probably govern the signal change. Considering that all samples provide the same average microparticle size, an increase in specific surface area, while the total pore volume stays unchanged, indicates an increase in surficial surface area of the supraparticles. Thus, the sensor molecule
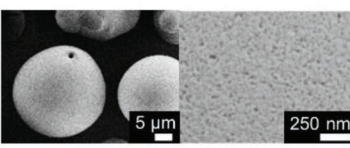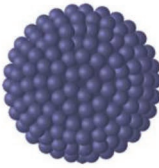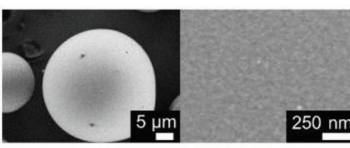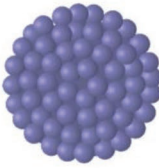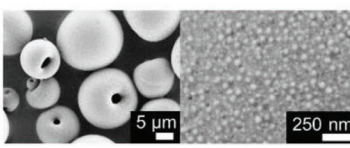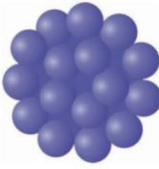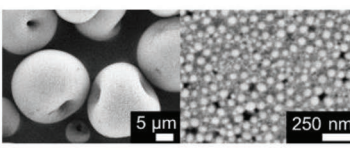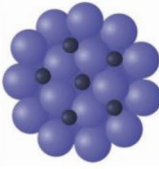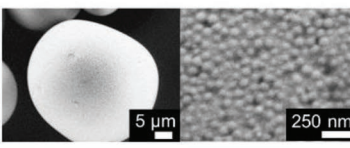
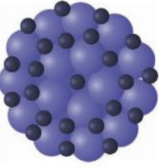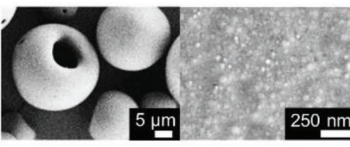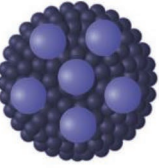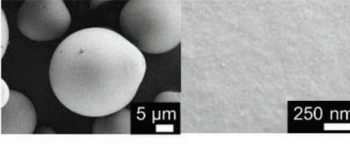| Sample denomination	Sketch	Primary nanoparticle size [nm]	Specific surface area [m² g⁻¹]	Average pore diameter [Å]	Total pore volume [cm³ g⁻¹]	SEM images
Particle A		7	85	77	0.163	
Particle B		10	135	47	0.159	
Particle C		35	60	107	0.159	
Particle D		95	46	160	0.185	
Particle E		10 and 95 ratio 1:9	56	108	0.150	
Particle F		10 and 95 ratio 5:5	107	47	0.125	
Particle G		10 and 95 ratio 9:1	166	37	0.156	

Figure 1. Overview of the seven indicator supraparticle supports ("Particle A" to "Particle G") studied in this work, which differ in terms of primary nanoparticle building block size (from 10 to 95 nm and mixtures of them).

concentration on the microparticle surface can be relatively higher and therefore, Particle B shows despite smaller pore diameters a higher gas sensitivity compared to Particle A.

For gas detection applications, the sensor response within the first 60 s of CO exposure (Figure 2d) is of particular importance as it determines the time delay between gas exposure and detection. A relative change of reflection of 2.5% is achieved within ≈20 s in the case of indicators containing Particles

C and D, while the one with Particle B requires around 50 s and with Particle A more than 1 min. As a finer tuning of the sensor response yielding reflection changes of 2.5% within 20 and 50 s would be very convenient, Particles E to G were synthesized. These supraparticles comprise mixtures of primary nanoparticles of 10 and 95 nm in size and are therefore expected to provide porosity values and specific surface areas between Particles D and B. Consequently, the relative change
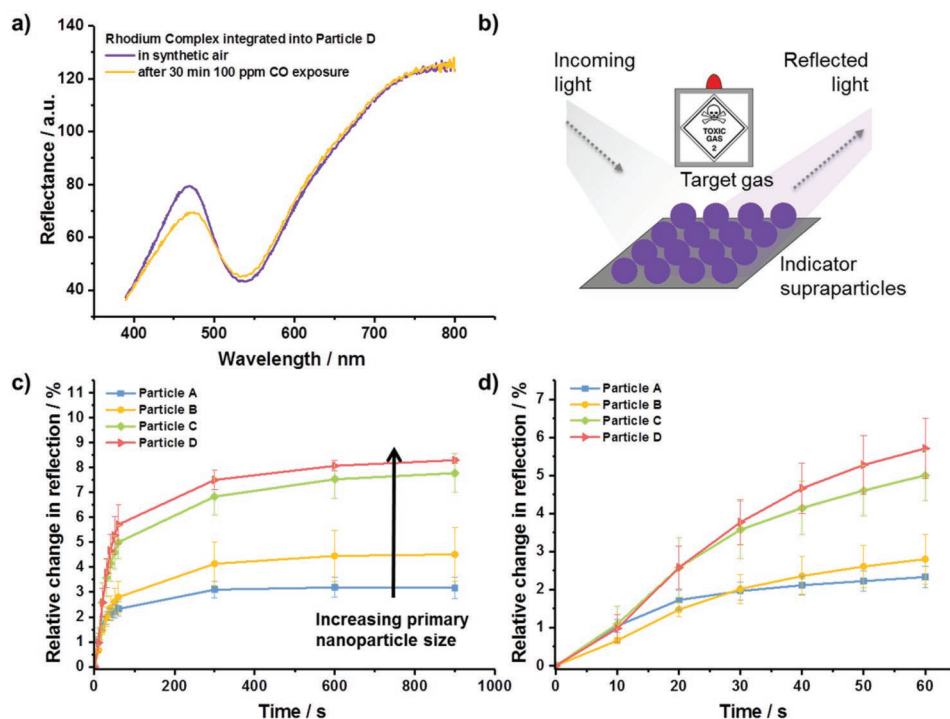
Figure 2. a) Reflectance spectra of the rhodium complex, integrated into Particle D, in absence and presence of CO. b) Reflection-based detection principle for measuring the response of indicator supraparticles to a target gas exposure. c) Relative change in reflection at 470 nm, indicating the color change of the rhodium complex containing indicator supraparticles (Particles A, B, C, and D), caused by exposure to 100 ppm CO for 15 min and d) showing the response of the sensor within the first 60 s of CO exposure. The primary nanoparticle sizes within the sensor supraparticles increase from particle sample A to D.

in reflection of the rhodium complex-containing Particles E to G at 15 min (**Figure 3**a) as well as at 60 s (Figure 3b) of CO exposure lie (dependent of the Particle B content) in-between the values of Particle D and Particle B. The response time (achieving a reflection change of 2.5%) is thus varied from around 20 s (Particle D) over 25 s (Particle E), 30–35 s (Particles F and G), and 50 s (Particle B) depending on the type of supraparticle.

2.3. NH₃ Sensing by Indicator Supraparticles

In order to show the flexibility of the supraparticles as support matrix for diverse sensing molecules, Particle D was loaded with Reichardt's dye. Loaded onto Particle D, this molecule shows a change in color (colorless to purple) in presence of NH_3. **Figure 4**a depicts the relative change in reflection of Reichardt's dye containing Particle D during 100 ppm NH_3
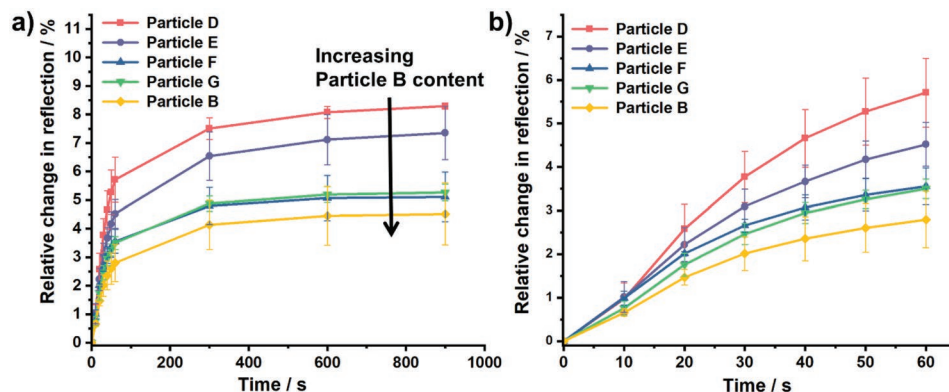
Figure 3. a) Relative change in reflection at 470 nm indicating the color change of the rhodium complex containing indicator supraparticles (Particles D, E, F, G, and B) caused by exposure to 100 ppm CO for 15 min and b) sensor response within the first 60 s of CO exposure. The percentage of primary nanoparticles with a size of 10 nm within the supraparticle increases compared to nanoparticles of 95 nm in size from particle sample E to G, while Particle D contains only 95 nm nanoparticles and Particle B contains only 10 nm nanoparticles.
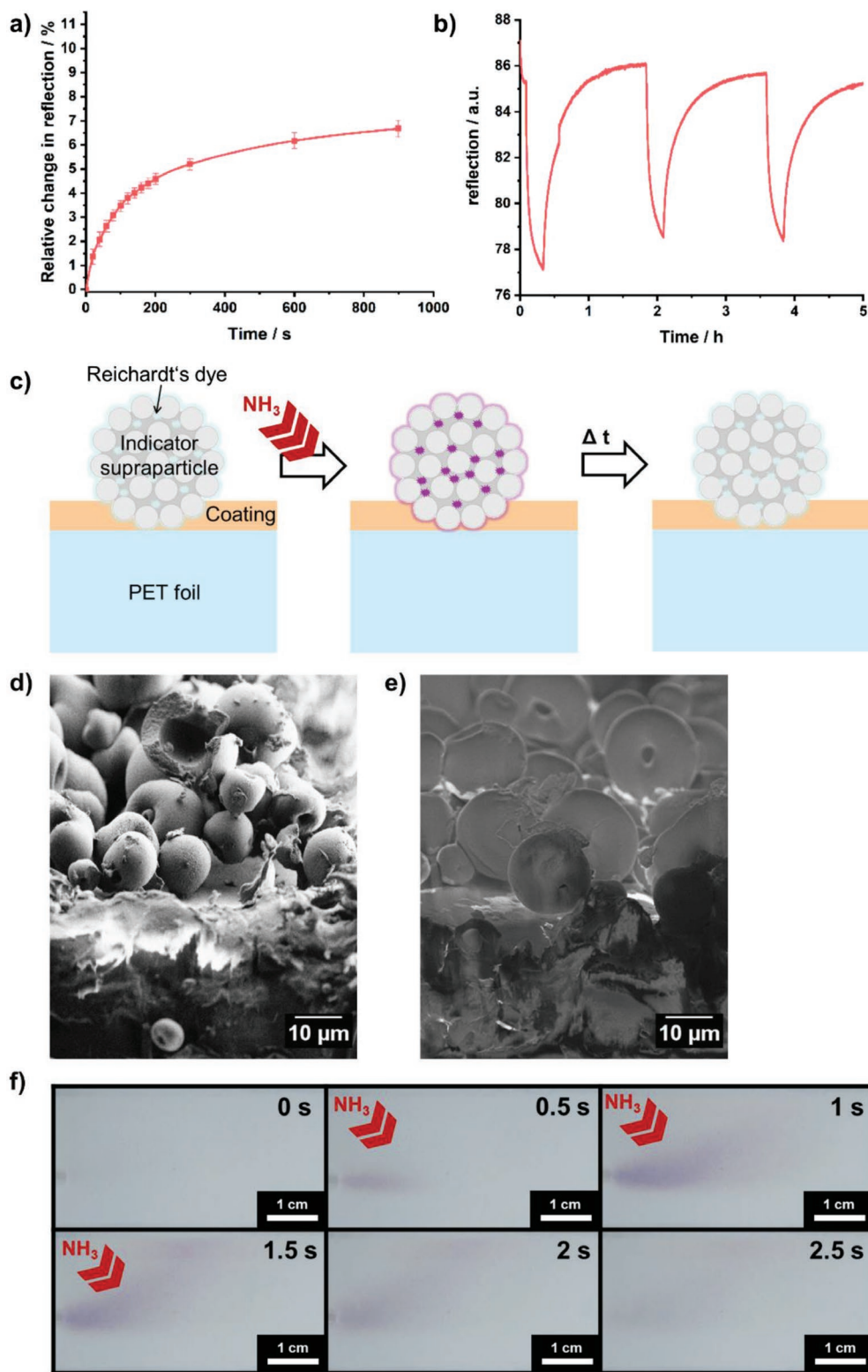
Figure 4. a) Relative change in reflection at 500 nm indicating the color change of the Reichardt's dye containing Particle D caused by exposure to 100 ppm NH_3 for 15 min and b) three cycles of NH_3 exposure and clean air flushing to demonstrate the reversibility of the sensor's color change. c) Scheme showing the Reichardt's dye containing supraparticle immobilized on a coating on PET foil and the NH_3 gas triggered color change as well as its time-dependent reconversion. Cross-sections of the indicator supraparticles on the coating of a PET foil acquired on an SEM via d) secondary electron detection and e) in-lens detection. f) Photo collection showing the NH_3 triggered color change and reconversion of the indicator supraparticles on the coating (for a video, see Video S1, Supporting Information).

gas exposure over 15 min. Although this indicator supraparticle comprises another sensing molecule, its sensitivity and response is similar to binary rhodium complex containing Particle D. This indicates that the sensing behavior of the indicator supraparticle is mainly influenced by its support matrix and not by the type of indicator dye.

Furthermore, the color reversibility as well as the sensing repeatability of the indicator supraparticle was shown via three gas exposure cycles (Figure 4b).

For the application of the indicator supraparticles in a gas detection device, their immobilization on a matrix material, e.g., a coating, is necessary. Therefore, as a proof of concept the Reichardt's dye containing Particle D was applied on a coating on flexible polyethylene terephthalate (PET) foil. Figure 4c depicts its schematic setup and the reversible NH_3 triggered color change of the indicator supraparticle. The micrometer-sized particles easily poke out of the thin coating layer enabling direct contact to the measured gas independent of the matrix material. SEM images (Figure 4d,e) clearly show the accessibility of the indicator supraparticles (while the thin coating layer fixing the microparticles cannot be distinguished from the PET foil). The gas triggered color change and its reconversion can be readily observed by the "naked eye" (Figure 4f, for a video, see the Supporting Information).

3. Conclusion

The herein presented silica supraparticles were assembled upon spray-drying and used as support matrix for sensing molecules such as Reichardt's dye and a binuclear rhodium complex for NH_3 and CO detection, respectively. The spray-drying technique affords high flexibility in primary particle size selection and thus, easy adjustment of the porosity and specific surface area of the obtained microparticles, which ultimately enables the fine-tuning of the sensor sensitivity and response. Due to their microscale size, they are large enough to poke out of thinner coating layers guaranteeing their gas accessibility independent of the coating material, while being small enough to be applicable to flexible substrates. The indicator supraparticle setup is simple, their production is inexpensive and upscalable, and their colorimetric changes can be observed by the "naked eye," even at low analyte concentrations.

4. Experimental Section

Reagents and Materials: Silica nanoparticles in the form of an aqueous nanoparticle dispersion containing 30 wt% silica with a hydrodynamic diameter of about 7 ± 2 nm (dynamic light scattering (DLS) measurements, Köstrosol K0730) and of about 10 ± 5 nm (K1030) were purchased from Chemiewerke Bad Köstritz (Germany) as well as dispersions, containing 50 wt% silica with a hydrodynamic diameter of 35 ± 5 nm (K3550) and 95 ± 5 nm (K9550), respectively. Reichardt's dye (2,6-diphenyl-4-(2,4,6-triphenyl-1-pyridinio)phenolate, $C_{41}H_{29}NO$) was purchased from Sigma-Aldrich (Germany). Rhodium acetate dimer (+98%), tris(3-fluorophenyl)phosphine (97%), Toluene (99%), and acetic acid (99%) were purchased from Sigma-Aldrich (Germany). All chemicals were used without further purification.

Synthesis of the Binuclear Rhodium Complex: Rhodium acetate dimer (618.4 mg) and tris(3-fluorophenyl)phosphine (2.8 mmol) were dissolved in 100 mL toluene. 20 mL of acetic acid were added and the reaction mixture was refluxed at 125 °C for 3 h. The solvent was removed to yield a deep purple solid.

Synthesis of Raspberry-Like Microparticles: In order to obtain nanostructured raspberry-like microparticles, the different silica nanoparticle dispersions were spray dried in various compositions with a "B-290" mini spray dryer from Büchi (Switzerland). The resulting supraparticles either contained a single nanoparticle primary size of 7, 10, 35, and 95 nm and were named as Particles A, B, C, and D, respectively (also see Figure 2), or mixtures of 10 and 95 nm primary particles with weight ratios of 1:9, 5:5, and 9:1 (referred to as Particles E, F, and G, respectively). The inlet air temperature was chosen to be 120 °C and the outlet temperature was 55–60 °C during the spray-drying process. After spray-drying, the produced powders were additionally dried in an oven at 110 °C for 48 h.

Synthesis of CO Indicator Supraparticles: In order to obtain CO indicator supraparticles, 200 mg of raspberry-like microparticles were weighed into a five milliliter round bottom flask. The binuclear rhodium complex was dissolved in toluene with a concentration of 0.3 wt%. 2.66 gm of the dye-toluene-solution was added to the round bottom flask, resulting in a dye to microparticle weight ratio of 1:25. The dye-microparticle-dispersion was stirred and shaken until the supernatant was colorless and the microparticles showed a deep purple color. The supernatant was taken off and the resulting dye modified microparticles were dried in a vacuum oven at 60 °C and a pressure of 10 mbar for 48 h. After drying, the CO indicator supraparticles showed a pink to purple color.

Synthesis of NH_3 Indicator Supraparticles: In order to obtain NH_3 indicator supraparticles, 200 mg of raspberry-like microparticles were weighed into a five milliliter round bottom flask. Reichardt's dye was dissolved in toluene with a concentration of 0.1 wt%. One gram of the dye-toluene-solution was added to the round bottom flask, resulting in a dye to microparticle weight ratio of 1:200. The dye-microparticle-dispersion was stirred and shaken until the supernatant was colorless and the microparticles showed a deep blue color. The supernatant was taken off and the resulting dye modified microparticles were dried in a vacuum oven at 60 °C and a pressure of 10 mbar for 48 h. After drying, the NH_3 indicator supraparticles were colorless.

Synthesis of a Coating with NH_3 Indicator Supraparticles: In order to obtain an NH_3-sensitive surface coating, a 100 µm PET substrate was coated with a lacquer using a 15 µm blade. The formulation of the lacquer consisting of 25% solids content in ethanol was prepared as described in refs. [24]. The NH_3 indicator supraparticles were spread on the still wet lacquer and evenly distributed on the lacquer by shaking. The excess particles were removed with compressed air. The curing was conducted thermally at 60 °C for 24 h. The approximated thickness of the obtained supraparticle coating was around 50 µm.

Characterization: The morphology of the raspberry-like supraparticles and the coating with NH_3 indicator supraparticles was studied via SEM on a Zeiss Supra 25 at 3 keV (field emission) and a secondary electron sensitive as well as an in-lens detector. Specific surface areas were measured by N_2 adsorption using BET analyses following DIN66131 with a Quantachrome Instruments Autosorb-3B on degassed and dried samples (110 °C, 10^{-3} mbar, 16 h). The average diameters of the supraparticles mesopores were estimated from the N_2 adsorption–desorption isotherms based on BJH analysis and the total pore volume was determined from the isotherms using the Gurvich rule. The sensor response under CO and NH_3 exposure in synthetic air at room temperature and 40% humidity was measured with a Perkin Elmer Lambda 900 UV–vis spectrometer, using a Praying Mantis reflection setup for probes with diffuse surfaces.[25] Each supraparticle size was measured three times. The probes were replaced after gas exposure.

Supporting Information

Supporting Information is available from the Wiley Online Library or from the author.

[1] K. Schmitt, K. Tarantik, C. Pannek, G. Sulz, J. Wöllenstein, *Procedia Eng.* **2016**, *168*, 1237.

[2] K. I. Oberg, R. Hodyss, J. L. Beauchamp, *Sens. Actuators, B* **2006**, *115*, 79.

[3] H. Greim, D. Bury, H.-J. Klimisch, M. Oeben-Negele, K. Ziegler-Skylakakis, *Chemosphere* **1997**, *36*, 271.

[4] E. H. Page, *Occup. Environ. Med.* **2003**, *60*, 69.

[5] M. E. Moragues, J. Esteban, J. V. Ros-Lis, R. Martínez-Máñez, M. D. Marcos, M. Martínez, J. Soto, F. Sancenón, *J. Am. Chem. Soc.* **2011**, *133*, 15762.

[6] M. E. Moragues, R. Montes-Robles, J. V. Ros-Lis, M. Alcañíz, J. Ibañez, T. Pardo, R. Martínez-Máñez, *Sens. Actuators, B* **2014**, *191*, 257.

[7] Y.-C. Chang, H. Bai, S.-N. Li, C.-N. Kuo, *Sensors* **2011**, *11*, 4060.

[8] K. Kanzawa, J. Kitano, *Proc. SEMI Adv. Semicond. Manuf. Conf. Workshop*, IEEE, Cambridge, MA, USA, 13–15 November, **1995**, pp. 190–193.

[9] M. T. Veciana-Nogués, A. Mariné-Font, M. C. Vidal-Carou, *J. Agric. Food Chem.* **1997**, *45*, 4324.

[10] C. Pannek, K. Schmitt, J. Wöllenstein, Transducers—2015 18th Int. Conf. Solid-State Sens., Actuators Microsyst., 21–25 June, Anchorage, Alaska, IEEE, Piscataway, NJ **2015**.

[11] W. N. Opdycke, S. J. Parks, M. E. Meyerhoff, *Anal. Chim. Acta* **1983**, *155*, 11.

[12] H. Hisamoto, H. Tohma, T. Yamada, K.-I. Yamauchi, D. Siswanta, N. Yoshioka, K. Suzuki, *Anal. Chim. Acta* **1998**, *373*, 271.

[13] S. Fiorilli, B. Onida, D. Macquarrie, E. Garrone, *Sens. Actuators, B* **2004**, *100*, 103.

[14] B. Onida, S. Fiorilli, L. Borello, G. Viscardi, D. Macquarrie, E. Garrone, *J. Phys. Chem. B* **2004**, *108*, 16617.

[15] D. Crowther, X. Liu, *J. Chem. Soc., Chem. Commun.* **1995**, 2445.

[16] P. Blum, G. J. Mohr, K. Matern, J. Reichert, U. E. Spichiger-Keller, *Anal. Chim. Acta* **2001**, *432*, 269.

[17] F. L. Dickert, U. Geiger, P. Lieberzeit, U. Reutner, *Sens. Actuators, B* **2000**, *70*, 263.

[18] C. Pannek, K. R. Tarantik, K. Schmitt, J. Wöllenstein, *Sensors* **2018**, *18*, 1994.

[19] K. Tarantik, K. Schmitt, C. Pannek, L. Miensopust, J. Wöllenstein, *Proceedings* **2017**, *1*, 454.

[20] S. Tao, L. Xu, J. C. Fanguy, *Sens. Actuators, B* **2006**, *115*, 158.

[21] S. Wintzheimer, T. Granath, M. Oppmann, T. Kister, T. Thai, T. Kraus, N. Vogel, K. Mandel, *ACS Nano* **2018**, *12*, 5093.

[22] P. Biswas, D. Sen, S. Mazumder, J. Ramkumar, *Colloids Surf., A* **2017**, *520*, 279.

[23] M. Oppmann, M. Wozar, J. Reichstein, K. Mandel, *ChemNanoMat* **2018**, *6*, 141.

[24] T. Ballweg, C. Gellermann, K. Mandel, *ACS Appl. Mater. Interfaces* **2015**, *7*, 24909.

[25] Harrick Scientific Product, Praying Mantis Data Sheet, https://www.harricksci.com/sites/default/files/pdf/data_sheets/Data_Sheet_Praying_Mantis.pdf (accessed: August 2019).